文章编号: 1000-324X(2022)09-0969-07 **DOI:** 10.15541/jim20210771

宽光谱透过 $Mg_{0.9}Al_{2.08}O_{3.97}N_{0.03}$ 透明陶瓷的制备与性能研究

李文俊, 王 皓, 涂兵田, 谌强国, 郑凯平, 王为民, 傅正义

(武汉理工大学 材料复合新技术国家重点实验室, 武汉 430070)

摘 要: $MgAl_2O_4$ 透明陶瓷具有优异的光学性能, 但其较差的机械性能和成型过程中的水解问题限制了实际应用, 通过组成设计 MgAlON 四元尖晶石可以有效调节其综合性能。本研究采用凝胶注模成型、无压烧结和热等静压处理制备了一种具有宽光谱透过范围的新型 $Mg_{0.9}Al_{2.08}O_{3.97}N_{0.03}$ 透明陶瓷, 系统比较其与 $MgAl_2O_4$ 透明陶瓷的光学性能和机械性能, 分析了低应力下裂纹的缓慢扩展并预测使用寿命。研究表明：固相体积分数为 50%的陶瓷浆料粘度最低, 为 124 mPa·s, 满足凝胶注模成型的需求; 2 mm 厚的 $Mg_{0.9}Al_{2.08}O_{3.97}N_{0.03}$ 透明陶瓷样品在 3.7 μm 处的直线透过率达 86.2%, 光学透过范围与 $MgAl_2O_4$ 相比拟, 折射率和阿贝数略高于 $MgAl_2O_4$; 同时, 该陶瓷具有和 $MgAl_2O_4$ 相近的 Weibull 模数, 尽管裂纹缓慢扩展系数比 $MgAl_2O_4$ 小, 但特征强度(210.6 MPa)和惰性强度(227.5 MPa)均高于 $MgAl_2O_4$。包含少量 N 的 MgAlON 尖晶石较好地克服了陶瓷粉体的水解问题, 并在保持优越光学性能的前提下显著提高了透明陶瓷的机械性能。本研究为尖晶石型透明陶瓷的制备与性能的改善提供了新的途径。

关 键 词: 透明陶瓷; 凝胶注模成型; 机械性能; 光学性能

中图分类号: TQ174 **文献标志码:** A

Preparation and Property of $Mg_{0.9}Al_{2.08}O_{3.73}N_{0.03}$ Transparent Ceramic with Broad Optical Transmission Range

LI Wenjun, WANG Hao, TU Bingtian, CHEN Qiangguo,
ZHENG Kaiping, WANG Weiming, FU Zhengyi

(State Key Laboratory of Advanced Technology for Materials Synthesis and Processing, Wuhan University of Technology, Wuhan 430070, China)

Abstract: $MgAl_2O_4$ transparent ceramics possess excellent optical property, but their practical applications are somewhat restricted by the hydrolysis problem during the shaping process and limited mechanical property. Meanwhile, it has been demonstrated that the property of quaternary MgAlON spinel can be effectively adjusted *via* varying their composition. Accordingly, a novel $Mg_{0.9}Al_{2.08}O_{3.97}N_{0.03}$ transparent ceramic with a broad transmittance range was prepared by combining aqueous gel-casting, pressureless sintering, and hot isostatic pressing treatment. Optical and mechanical property of this transparent ceramic were systematically investigated and compared with

收稿日期: 2021-12-17; **收到修改稿日期:** 2022-02-22; **网络出版日期:** 2022-06-16

基金项目: 国家重点研发计划(2017YFB0310500); 国家自然科学基金(51472195); 三亚科教创新园开放基金(2020KF0018)
National Key Research and Development Program of China (2017YFB0310500); National Natural Science Foundation of China (51472195); Sanya Science and Education Innovation Park Open Fundation (2020KF0018)

作者简介: 李文俊(1996–), 男, 硕士研究生. E-mail: 15826911464@163.com
LI Wenjun (1996–), male, Master candidate. E-mail: 15826911464@163.com

通信作者: 王 皓, 教授. E-mail: shswangh@whut.edu.cn
WANG Hao, professor. E-mail: shswangh@whut.edu.cn

those of $MgAl_2O_4$ transparent ceramic. Furthermore, the slow crack growth under low stress were analyzed, and the service life of transparent ceramic was predicted. It is shown that the viscosity of ceramic slurry with 50% (in volume) solid load was 124 mPa·s, which could meet the requirement of aqueous gel-casting. The in-line transmittance of 86.2% at 3.7 μm was obtained in the $Mg_{0.9}Al_{2.08}O_{3.97}N_{0.03}$ transparent ceramic sample with thickness of 2 mm, and the optical transmittance range was comparable to that of $MgAl_2O_4$, with slightly higher refractive index and Abbé number. Further, this ceramic showed a Weibull modulus similar to $MgAl_2O_4$, and although its crack slow growth coefficient is lower than $MgAl_2O_4$, but both the characteristic strength (210.6 MPa) and inert strength (227.5 MPa) were much higher. Therefore, in the quaternary MgAlON spinel with low nitrogen content, the hydrolysis problem of ceramic powders could be well overcome, while the mechanical property of transparent ceramic was remarkably improved without degradation of optical property. This research provides a new pathway toward obtaining the novel spinel transparent ceramics with improved preparation and property.

Key words: transparent ceramics; aqueous gel-casting; mechanical property; optical property

$MgAl_2O_4$透明陶瓷是一种在0.3~5.5 μm波段具有重要应用的光学材料, 其光学透过范围在 0.11~7 μm, 理论透过率可达到 87%, 适用于红外窗口、条形码扫描仪及夜视系统等领域[1-4]。然而该材料的抗弯强度约为 150 MPa, 断裂韧性通常低于 2 $MPa·m^{1/2}$[5], 迫切需要在保持优异光学性能的同时提升材料的机械性能。目前, 减少烧结助剂用量和细化晶粒尺寸是改善 $MgAl_2O_4$ 透明陶瓷机械性能的主要手段[6-8], 但容易对材料的光学性能产生不利影响。另外, $MgAl_2O_4$ 粉体易产生水解行为, 难以通过水基凝胶注模成型制备高强度的大尺寸陶瓷[9-11]。如何获得综合性能优异且易于制备的尖晶石型透明陶瓷仍是亟待解决的问题。

MgAlON 是一种四元尖晶石固溶体, 其中无序混合的O^{2-}和N^{3-}呈面心紧密堆积, Mg^{2+}和Al^{3+}分布于四面体和八面体空隙。MgAlON 晶体结构复杂、组成变化范围宽, 可在较大范围内调控材料性能[12-13]。Liu 等[14]采用无压烧结制备了 $Mg_{0.27}Al_{2.58}O_{3.73}N_{0.27}$ 透明陶瓷, 发现该陶瓷的光学透过范围介于 AlON 和 *c* 面蓝宝石之间。Zhang 等[15]系统评价了该透明陶瓷的机械性能, 其显著优于 $MgAl_2O_4$。Zong 等[16]还发现 $Mg_{0.27}Al_{2.58}O_{3.73}N_{0.27}$ 粉体不会发生水解, 适合用水基凝胶注模成型制备大尺寸、复杂形状的部件。Zong 等[13]通过材料组成设计与调控, 制备出一种光学透过域与 *c* 面蓝宝石相当的新型 $Mg_{0.55}Al_{2.36}O_{3.81}N_{0.19}$ 透明陶瓷。上述研究表明, 随着 MgAlON 透明陶瓷中 N 含量降低和 Mg 含量上升, 陶瓷的光谱透过范围变宽, 且机械性能始终优于 $MgAl_2O_4$, 同时还易于水基胶态成型。

本研究通过调控组成设计与晶体结构, 采用高温固相反应合成 $Mg_{0.9}Al_{2.08}O_{3.97}N_{0.03}$ 陶瓷粉体, 通过凝胶注模成型、无压烧结结合热等静压处理制备透明陶瓷。研究陶瓷浆料的流变学性能, 评价 $Mg_{0.9}Al_{2.08}O_{3.97}N_{0.03}$ 透明陶瓷的光学性能和机械性能, 进而分析该陶瓷的裂纹扩展情况和疲劳特性。

1 实验方法

以高纯度的 α-Al_2O_3、AlN 和实验室自制的 $MgAl_2O_4$ 为原料, 经过高温固相反应制得单相 $Mg_{0.9}Al_{2.08}O_{3.97}N_{0.03}$ 粉体。然后通过水基凝胶注模成型制备陶瓷坯体, 具体过程如下: 以甲基丙烯酰胺(MAM, 98%, Ourchem Chem, 中国)作为单体, *N*, *N*′-亚甲基双丙烯酸酰胺(MBAM, 97%, Alfa Aesar Chem, 美国)作为交联剂, 柠檬酸三铵(TAC, 97%, Alfa Aesar Chem, 美国)作为分散剂, 搅拌 2 h 制得固相体积分数为 50%的浆料, 随后加入体积分数 1%的引发剂过硫酸铵(APS, 98%, Alfa Aesar Chem, 美国)并真空搅拌除泡 30 min, 加入体积分数 0.25%的催化剂 *N*, *N*, *N*′, *N*′-四甲基乙烯二胺(TEMED, 99%, Alfa Aesar Chem, 美国), 再把浆料注入到模具中使之固化成型获得陶瓷坯体。脱模后将坯体置于室温下干燥 48 h, 冷等静压(200 MPa, 5 min)后在马弗炉中加热至 630 ℃以排除有机物。将坯体在 1.01×10^5 Pa N_2 气氛下 1675 ℃保温 2 h, 所得陶瓷预烧体在 180 MPa Ar 气氛中 1800 ℃热等静压烧结 5 h, 然后对样品进行切割、两面研磨和抛光, 备用。

使用 X 射线衍射仪(Model χ'Pert PRO of Panalytical, Almelo, 荷兰)对粉体和陶瓷的物相进行鉴定。通过旋转黏度计(Brookfield Viscometer, 美国)

测试浆料的流变学性能, 剪切速率范围为 0.01~56 s^{-1}。用氧氮分析仪(TC600, Leco, 美国)和电感耦合等离子体原子发射光谱(ICP-AES Optima4300DV, PerkinElmer, 美国)确定粉体的实际组成; 使用扫描电子显微镜(Hitachi S-3400N,日本)观察坯体、陶瓷断口及刻蚀表面的形貌特征, 其中表面抛光的陶瓷样品在 200 ℃的浓磷酸中刻蚀 15 min。分别采用紫外–近红外分光光度计(Lambda750 S, PerkinElmer, 美国)和智能傅里叶红外光谱仪(Model Nexus, Thermo Nicolet Corporation, Madison, WI)测试透明陶瓷样品在 200~2500 nm 和 2500~7000 nm 范围的光学直线透过率; 通过椭圆偏振光谱仪(M-2000V, J.A. Woollam, 美国)测试样品在不同波长下的折射率。用维氏硬度计(Model 430 SVD, Wolpert, 中国)测试样品的维氏硬度、测试载荷 9.8 N、保压时间 15 s; 利用压痕法测试样品的断裂韧性; 使用弹性模量测试仪(GrindoSonic MK7, GrindoSonic, 比利时)测量样品的杨氏模量, 测试方法为脉冲激励法; 采用万能试验机(MTS810 100KN, MTS, 美国)测量陶瓷的抗弯强度, 测试方法为四点弯曲法[17](GB/T 6569-2006, 样品尺寸为 3 mm×4 mm×35 mm)。利用热膨胀仪(DIL402SE, Netzsch, 德国)测定样品的热膨胀系数。

2　结果与讨论

2.1　$Mg_{0.9}Al_{2.08}O_{3.97}N_{0.03}$ 透明陶瓷的制备

通过氧氮分析仪结合 ICP-AES 测定陶瓷粉体的实际组成为 $Mg_{0.9}Al_{2.08}O_{3.97}N_{0.03}$, 与设计组成($Mg_{0.94}Al_{2.05}O_{3.98}N_{0.02}$)差别不大, 差别主要来源于 Mg、N 的少量挥发[18]。图 1(a)是所得粉体和陶瓷预烧体的 XRD 图谱, 从图中可以看到, 粉体和陶瓷的衍射峰位置均与尖晶石的 PDF#99-0098 标准卡片一一对应, 说明它们是由单一尖晶石相组成。

图 1(b)显示了固相体积分数为 50%时, 分散剂含量对浆料黏度的影响。在剪切速率 50 s^{-1} 下, TAC 质量分数为 0.4%时, 浆料的黏度最低, 为 124 mPa·s, 说明该浆料可满足水基凝胶注模成型制备陶瓷坯体的要求。

从图 1(c)可以看到, 坯体中陶瓷颗粒堆积较紧密、分布较均匀, 粒径约为 0.4 μm。图 1(d)是热等静压烧结后样品的表面 SEM 照片, 平均晶粒尺寸约为 100 μm、没有出现晶粒的异常长大, 但是残留少量的小气孔。

2.2　光学性能

图 2(a)为 $Mg_{0.9}Al_{2.08}O_{3.97}N_{0.03}$、$MgAl_2O_4$ 透明陶瓷、c 面蓝宝石[1]和 $Mg_{0.27}Al_{2.58}O_{3.73}N_{0.27}$ 透明陶瓷[14]的光学透过谱。从插图中可以看到, 制备的样品表观透光性良好。2 mm 厚的 $Mg_{0.9}Al_{2.08}O_{3.97}N_{0.03}$ 陶瓷样品在 3.7 μm 处的透过率为 86.2%, 在可见光波段样品的透过率略低于 $MgAl_2O_4$ 透明陶瓷, 这是因为陶瓷中残留少量的小气孔(图 1(d))。最终样品的光谱透过范围为 0.2~6.7 μm, 与 $MgAl_2O_4$ 透明陶瓷接近, 较 c 面蓝宝石和 $Mg_{0.27}Al_{2.58}O_{3.73}N_{0.27}$ 陶瓷更宽。在尖晶石晶体中, 随着 Mg 含量增大和 N 含量降低, 晶格振动频率降低, 声子吸收红移, 光谱透过范围变宽[13]。

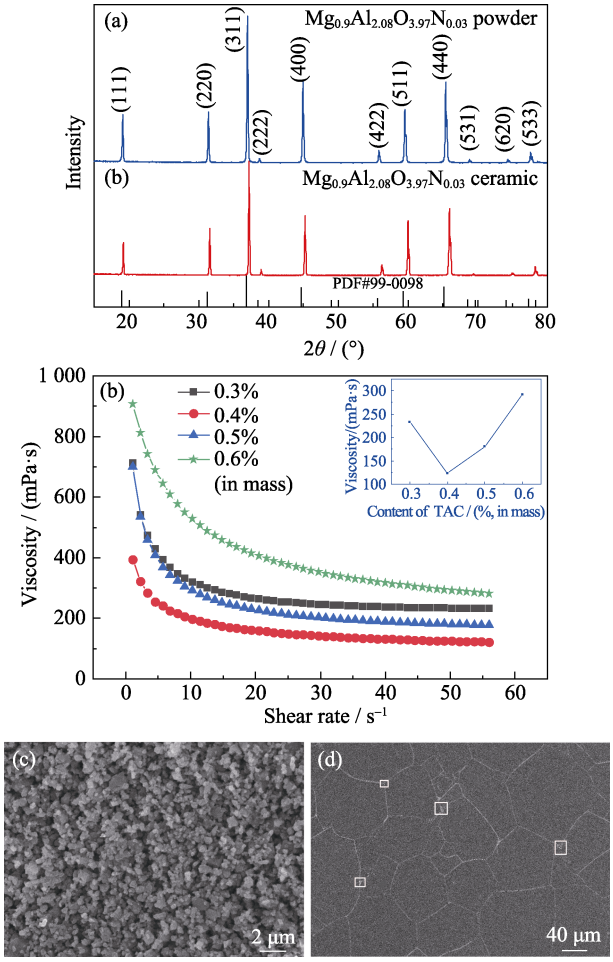

图 1　$Mg_{0.9}Al_{2.08}O_{3.97}N_{0.03}$ 陶瓷粉体、浆料、坯体以及透明陶瓷的表征

Fig. 1　Characterization of $Mg_{0.9}Al_{2.08}O_{3.97}N_{0.03}$ powder, slurry, green body, and transparent ceramic

(a) XRD patterns of powder and ceramic; (b) Relationship between viscosity of slurry and contents of TAC; (c) Morphology of green body; (d) SEM image of etched surface of transparent ceramic

采用 Sellmeier 方程[20]对不同波长(λ)下透明陶瓷的折射率(n)进行拟合, 发现 n 与 λ 符合公式(1)关系:

$$n^2-1=\frac{3.79\lambda^2}{\lambda^2-130.03^2}+\frac{-1.9\lambda^2}{\lambda^2-152.48^2} \quad (1)$$

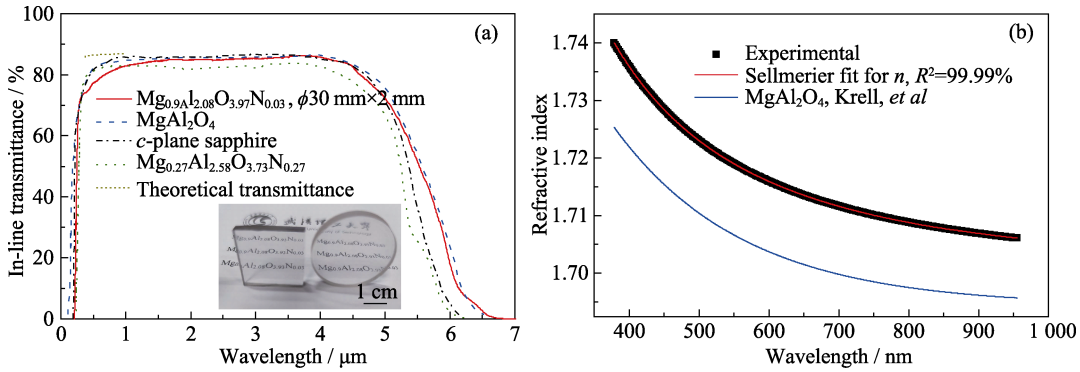

图 2 透明陶瓷光学性能比较

Fig. 2 Comparison of optical property of transparent ceramics

(a) In-line transmittance of $Mg_{0.9}Al_{2.08}O_{3.97}N_{0.03}$, $MgAl_2O_4$, *c*-plane sapphire[1], $Mg_{0.27}Al_{2.58}O_{3.73}N_{0.27}$ transparent ceramics[14]; (b) Refractive index of $Mg_{0.9}Al_{2.08}O_{3.97}N_{0.03}$, $MgAl_2O_4$ transparent ceramics[19]

从图 2(b)中可见，$Mg_{0.9}Al_{2.08}O_{3.97}N_{0.03}$ 透明陶瓷的折射率略大于 $MgAl_2O_4$[19]。这是因为 N^{3-}的电子极化率大于 O^{2-}，同时 $Mg_{0.9}Al_{2.08}O_{3.97}N_{0.03}$ 的晶胞体积略小于 $MgAl_2O_4$。根据折射率曲线，采用式(2)计算阿贝数(v)[21]，用于描述材料的色散。

$$v=\frac{n_D-1}{n_F-n_C} \tag{2}$$

其中，n_D、n_F、n_C 分别表示材料在 589.3、486.1 和 656.3 nm 处的折射率。由此计算出的阿贝数为 65.27，比 $MgAl_2O_4$ 透明陶瓷(60.67)[19]略大，说明 $Mg_{0.9}Al_{2.08}O_{3.97}N_{0.03}$ 透明陶瓷的色散更轻微。

2.3 断裂强度的 Weibull 统计分析

采用四点弯曲法测量 $Mg_{0.9}Al_{2.08}O_{3.97}N_{0.03}$ 透明陶瓷的抗弯强度，样本数量为 30，利用两参数 Weibull 统计模型对抗弯强度数据进行统计处理[22-24]。材料断裂概率 P 为：

$$P=1-\exp\left[-\left(\frac{\sigma}{\sigma_N}\right)^m\right] \tag{3}$$

其中，σ 是材料的实测强度，σ_N 是材料的特征强度，m 是材料的 Weibull 模数。

图 3(a)是 $Mg_{0.9}Al_{2.08}O_{3.97}N_{0.03}$ 透明陶瓷的两参数 Weibull 统计分布图，可以看到对样品的实测强度线性拟合较好。从拟合结果可得，$Mg_{0.9}Al_{2.08}O_{3.97}N_{0.03}$ 透明陶瓷的 Weibull 模数为 5.97±0.25，特征强度为 210.6 MPa。文献[25]报道了 $MgAl_2O_4$ 透明陶瓷(平均晶粒尺寸约为 5 μm，下同)的 Weibull 模数为 5±2，特征强度为 169 MPa；而 $Mg_{0.27}Al_{2.58}O_{3.73}N_{0.27}$ 透明陶瓷[15]的 Weibull 模数为 4.5，特征强度为 255.54 MPa。本研究的材料特征强度介于 $MgAl_2O_4$ 和 $Mg_{0.27}Al_{2.58}O_{3.73}N_{0.27}$ 透明陶瓷之间，但 Weibull 模数高于它们。这说明在相同载荷下，$Mg_{0.9}Al_{2.08}O_{3.97}N_{0.03}$ 陶瓷的断裂概率比 $MgAl_2O_4$ 低。造成这三种材料特征强度和 Weibull 模数差异的原因可能来自于它们组成和显微结构的不同[26]。

图 3(b)是 $Mg_{0.9}Al_{2.08}O_{3.97}N_{0.03}$ 陶瓷的断口形貌，可以看出，样品中存在明显的穿晶和沿晶混合断裂过程以及台阶式断层，具备陶瓷的脆性断裂特

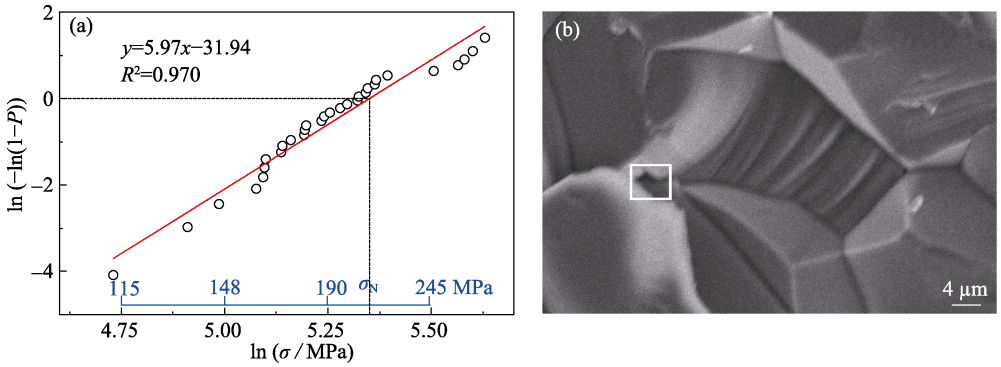

图 3 $Mg_{0.9}Al_{2.08}O_{3.97}N_{0.03}$ 透明陶瓷的抗弯强度 Weibull 统计图(a)和断面 SEM 照片(b)

Fig. 3 Weibull plot of fracture strength (a) and SEM image of fractured surface (b) of $Mg_{0.9}Al_{2.08}O_{3.97}N_{0.03}$ transparent ceramic

征，晶界处的小气孔可能是该材料的断裂源。

2.4　裂纹缓慢扩展

基于陶瓷材料在长时间、低应力下发生裂纹扩展的行为，研究不同载荷速率下 $Mg_{0.9}Al_{2.08}O_{3.97}N_{0.03}$ 透明陶瓷的四点抗弯强度。材料在低应力下微裂纹扩展对抗弯强度的影响可采用下式进行表征[28]：

$$\lg\sigma_f=\frac{1}{n'+1}\lg v+\lg D \tag{4}$$

其中，σ_f 是材料的抗弯强度，n' 是裂纹缓慢扩展系数，D 为材料的惰性强度，v 是载荷加载速率。

图 4(a)为不同加载速率下 $Mg_{0.9}Al_{2.08}O_{3.97}N_{0.03}$ 和 $MgAl_2O_4$ 透明陶瓷[27]的抗弯强度，可以看到，随着加载速率增大，透明陶瓷的抗弯强度均增大，这是由于加工后的透明陶瓷表面存在缺陷和损伤微裂纹，而脆性陶瓷的亚临界裂纹扩展导致在载荷作用下强度随作用时间的延长而降低[5]。根据公式(4)可以得出 $Mg_{0.9}Al_{2.08}O_{3.97}N_{0.03}$ 透明陶瓷的 n'≈20，D≈227.5 MPa；$MgAl_2O_4$ 透明陶瓷[27]的 n'≈50，D≈140 MPa，而 $Mg_{0.27}Al_{2.58}O_{3.73}N_{0.27}$ 透明陶瓷[15]的 n'≈11，n'≈270 MPa。这可能是因为 $Mg_{0.9}Al_{2.08}O_{3.97}N_{0.03}$ 透明陶瓷的晶粒尺寸大于 $MgAl_2O_4$ 陶瓷，但小于 $Mg_{0.27}Al_{2.58}O_{3.73}N_{0.27}$ 陶瓷，而晶粒尺寸小的陶瓷显微结构更均匀，裂纹不易在外应力的作用下扩展，n' 值就更大[29]。此外，$Mg_{0.9}Al_{2.08}O_{3.97}N_{0.03}$ 和 $Mg_{0.27}Al_{2.58}O_{3.73}N_{0.27}$ 透明陶瓷[15]的惰性强度均远高于 $MgAl_2O_4$ 透明陶瓷，这可能是由于它们的组成不同导致的惰性强度差异。

在实际应用中，陶瓷的使用寿命是一个非常重要的性能指标。将抗弯强度的 Weibull 统计结果和裂纹缓慢扩展相结合[27]，可得到表征陶瓷疲劳特性的关系式。

$$\ln(-\ln(1-P))=m\ln\sigma-m\ln\left(D\sqrt[n']{\frac{D}{t}}\right) \tag{5}$$

其中，t 是陶瓷的使用时间，其它参数含义同上。

为了预测材料在不同使用时间下的实际强度和失效概率，基于式(5)获得 $Mg_{0.9}Al_{2.08}O_{3.97}N_{0.03}$ 和 $MgAl_2O_4$ 透明陶瓷[27]的强度–概率–时间(Strength-probability-time, SPT)关系图。从图 4(b)中可以看出，材料的断裂概率为 63.2%时，随着使用时间从 1 s 延长到 10 a，$Mg_{0.9}Al_{2.08}O_{3.97}N_{0.03}$ 透明陶瓷对应的承受应力从 298 MPa 降低到 112 MPa。这说明随着材料使用时间延长，裂纹缓慢扩展导致材料可承受的应力降低。当 $Mg_{0.9}Al_{2.08}O_{3.97}N_{0.03}$ 和 $MgAl_2O_4$ 透明陶瓷都使用 10 a 后，$Mg_{0.9}Al_{2.08}O_{3.97}N_{0.03}$ 在应力 112 MPa 下断裂概率为 63.2%，而 $MgAl_2O_4$ 在该应力下的断裂概率超过 99%。这是因为 $Mg_{0.9}Al_{2.08}O_{3.97}N_{0.03}$ 透明陶瓷的惰性强度远大于 $MgAl_2O_4$ 透明陶瓷，不易在外应力冲击下破坏。因此在实际应用中，$Mg_{0.9}Al_{2.08}O_{3.97}N_{0.03}$ 透明陶瓷的使用寿命更长，适用于更苛刻的工作环境。

表 1 给出了 $Mg_{0.9}Al_{2.08}O_{3.97}N_{0.03}$ 和 $MgAl_2O_4$ 透明陶瓷的其它相关性能，从表中可以看到，$Mg_{0.9}Al_{2.08}O_{3.97}N_{0.03}$ 透明陶瓷的硬度、断裂韧性和杨氏模量略高于 $MgAl_2O_4$；热膨胀系数略低于 $MgAl_2O_4$ 透明陶瓷。这是因为两者组成和结构不同，随着尖晶石晶体中 Mg 含量增大和 N 含量减少，其四面体键的硬度和键力常数急剧下降，而八面体键的硬度和键力常数几乎不变，因此硬度、断裂韧性和杨氏模量降低[34]。

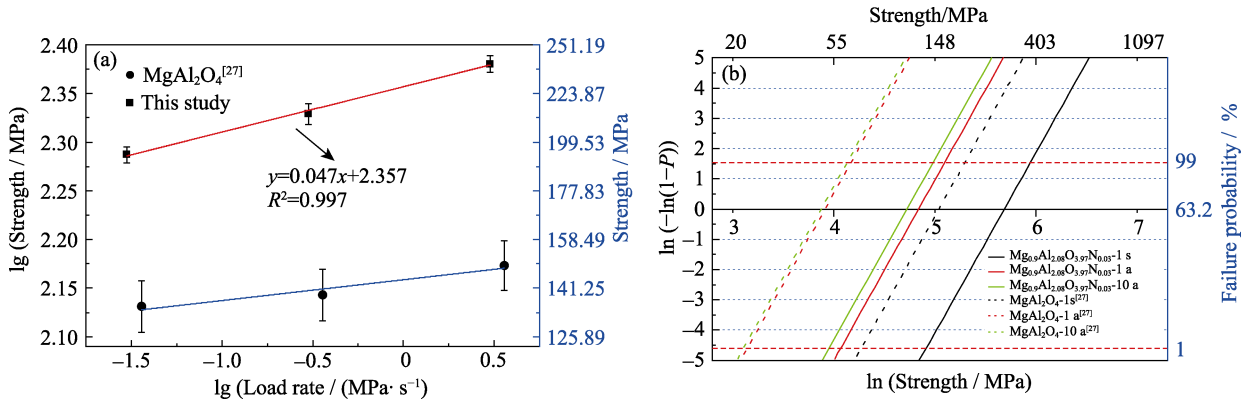

图 4　$Mg_{0.9}Al_{2.08}O_{3.97}N_{0.03}$ 和 $MgAl_2O_4$ 透明陶瓷[27]在不同载荷速率下的抗弯强度(a)与强度–概率–时间关系图(b)

Fig. 4　Fractured strength under different load rates (a) and strength-probability-time diagram (b) of $Mg_{0.9}Al_{2.08}O_{3.97}N_{0.03}$ and $MgAl_2O_4$[27] transparent ceramics

Colorful figures are available on website

表 1 $Mg_{0.9}Al_{2.08}O_{3.97}N_{0.03}$ 和 $MgAl_2O_4$ 透明陶瓷的性能

Table 1 Property of $Mg_{0.9}Al_{2.08}O_{3.97}N_{0.03}$ and $MgAl_2O_4$ transparent ceramic

Sample	Vickers hardness/GPa	Fracture toughness/(MPa·m$^{1/2}$)	Young's modulus/GPa	Thermal expansion coefficient/($\times10^{-6}$, K^{-1})
$MgAl_2O_4$[30-33]	12.9±0.49	1.6±0.1	273	6.97
$Mg_{0.9}Al_{2.08}O_{3.97}N_{0.03}$	13.7±0.12	2.12±0.1	280	6.57

3 结论

采用水基凝胶注模成型、无压预烧结合热等静压烧结制备了新型 $Mg_{0.9}Al_{2.08}O_{3.97}N_{0.03}$ 透明陶瓷。所得浆料的固相量高、粘度低, 适合水基凝胶注模成型制备陶瓷坯体。2 mm 厚的陶瓷样品在 3.7 μm 处的直线透过率达 86.2%, 且具有与 $MgAl_2O_4$ 透明陶瓷可比拟的光学透过域(0.2~6.7 μm)和略大的阿贝数。通过抗弯强度的 Weibull 统计以及裂纹缓慢扩展研究, 发现 $Mg_{0.9}Al_{2.08}O_{3.97}N_{0.03}$ 透明陶瓷的 Weibull 模数、特征强度和惰性强度均大于 $MgAl_2O_4$ 透明陶瓷, 但是裂纹缓慢扩展系数略小。另外, 较高的惰性强度使 $Mg_{0.9}Al_{2.08}O_{3.97}N_{0.03}$ 透明陶瓷的使用寿命更长。

参考文献:

[1] RUBAT D M, KLEEBE H J, MÜLLER M M, *et al*. Fifty years of research and development coming to fruition; unraveling the complex interactions during processing of transparent magnesium aluminate ($MgAl_2O_4$) spinel. *Journal of the American Ceramic Society*, 2013, **96(11):** 3341–3365.

[2] WAETZIG K, KRELL A, TRICE R. The effect of composition on the optical properties and hardness of transparent Al-rich MgO·$n$$Al_2O_3$ spinel ceramics. *Journal of the American Ceramic Society*, 2015, **99(3):** 946–953.

[3] SANGHERA J, BAYYA S, VILLALOBOS G, *et al*. Transparent ceramics for high-energy laser systems. *Optical Materials*, 2011, **33(3):** 511–518.

[4] PAPPAS J M, DONG X Y. Porosity characterization of additively manufactured transparent $MgAl_2O_4$ spinel by laser direct deposition. *Ceramics International*, 2020, **46(5):** 6745–6755.

[5] SALEM J A, SGLAVO V. Transparent armor ceramics as spacecraft windows. *Journal of the American Ceramic Society*, 2013, **96(1):** 281–289.

[6] ROTHMAN A, KALABUKHOV S, SVERDLOV N, *et al*. The effect of grain size on the mechanical and optical properties of spark plasma sintering-processed magnesium aluminate spinel $MgAl_2O_4$. *International Journal of Applied Ceramic Technology*, 2014, **11(1):** 146–153.

[7] SOKOL M, KALABUKHOV S, SHNECK R, *et al*. Effect of grain size on the static and dynamic mechanical properties of magnesium aluminate spinel ($MgAl_2O_4$). *Journal of the European Ceramic Society*, 2017, **37(10):** 3417–3424.

[8] NECINA V, PABST W. Grain growth of $MgAl_2O_4$ ceramics with LiF and NaF addition. *Open Ceramics*, 2021, **5(2):** 100078.

[9] ZHANG H, WANG H, GU H, *et al*. Preparation of transparent MgO·1.8Al_2O_3 spinel ceramics by aqueous gelcasting, presintering and hot isostatic pressing. *Journal of the European Ceramic Society*, 2018, **38(11):** 4057–4063.

[10] YAN J, YAN W, CHEN Z, *et al*. A strategy for controlling microstructure and mechanical properties of microporous spinel ($MgAl_2O_4$) aggregates from magnesite and $Al(OH)_3$. *Journal of Alloys and Compounds*, 2022, **896:** 163088.

[11] ZHANG P, LIU P, SUN Y, *et al*. Microstructure and properties of transparent $MgAl_2O_4$ ceramic fabricated by aqueous gelcasting. *Journal of Alloys and Compounds*, 2016, **657:** 246–249.

[12] WILLEMS H X, WITH G D, METSELAAR R. Thermodynamics of AlON III: stabilization of AlON with MgO. *Journal of the European Ceramic Society*, 1993, **12(1):** 43–49.

[13] ZONG X, WANG H, GU H, *et al*. A novel spinel-type $Mg_{0.55}Al_{2.36}O_{3.81}N_{0.19}$ transparent ceramic with infrared transmittance range comparable to *c*-plane sapphire. *Scripta Materialia*, 2020, **178(15):** 428–432.

[14] LIU X, WANG H, TU B T, *et al*. Highly transparent $Mg_{0.27}Al_{2.58}O_{3.73}N_{0.27}$ ceramic prepared by pressureless sintering. *Journal of the American Ceramic Society*, 2014, **97(1):** 63–66.

[15] ZHANG Z, WANG H, TU B T *et al*. Characterization and evaluation on mechanical property of $Mg_{0.27}Al_{2.58}O_{3.73}N_{0.27}$ transparent ceramic. *Journal of Inorganic Materials*, 2018, **33(9):** 1006–1010.

[16] ZONG X, WANG H, GU H, *et al*. Highly transparent $Mg_{0.27}Al_{2.58}O_{3.73}N_{0.27}$ ceramic fabricated by aqueous gelcasting, pressureless sintering, and post-HIP. *Journal of the American Ceramic Society*, 2019, **102(11):** 6507–6516.

[17] GB/T 6569-2006, 精细陶瓷弯曲强度试验方法.

[18] GRANON A, GOEURIOT P, THEVENOT F, *et al*. Reactivity in the Al_2O_3-AlN-MgO system. The MgAlON spinel phase. *Journal of the European Ceramic Society*, 1994, **13(4):** 365–370.

[19] KRELL A, HUTZLER T, KLIMKE J. Transmission physics and consequences for materials selection, manufacturing, and applications. *Journal of the European Ceramic Society*, 2009, **29(2):** 207–221.

[20] WEMPLE S H, DIDOMENICO M J. Behavior of the electronic dielectric constant in covalent and ionic materials. *Physical Review B*, 1971, **3(4):**1338–1351.

[21] CAI B, KAINO T, SUGIHARA O. Sulfonyl-containing polymer and its alumina nanocomposite with high Abbe number and high refractive index. *Optical Materials Express*, 2015, **5(5):** 1210–1216.

[22] KLEIN C A. Flexural strength of infrared-transmitting window materials: bimodal Weibull statistical analysis. *Optical Engineering*, 2011, **50(2):** 1–10.

[23] DENG B, JIANG D, GONG J. Is a three-parameter Weibull function really necessary for the characterization of the statistical variation of the strength of brittle ceramics? *Journal of the European Ceramic Society*, 2018, **38(4):** 2234–2242.

[24] KHALILI A. Statistical properties of Weibull estimators. *Journal of Materials Science*, 1991, **26:** 6741–6752.

[25] TOKARIEV O, SCHNETTER L, BECK T, *et al*. Grain size effect on the mechanical properties of transparent spinel ceramics. *Journal*

of the European Ceramic Society, 2013, **33(4):** 749–757.

[26] MALZBENDER J, STEINBRECH R W. Threshold fracture stress of thin ceramic components. *Journal of the European Ceramic Society*, 2008, **28(1):** 247–252.

[27] TOKARIEV O, STEINBRECH R W, SCHNETTER L, *et al*. Micro- and macro-mechanical testing of transparent $MgAl_2O_4$ spinel. *Journal of Materials Science*, 2012, **47:** 4821–4826.

[28] CHOI S R. Slow crack growth analysis of brittle materials with finite thickness subjected to constant stress-rate flexural loading. *Journal of Materials Science*, 1999, **34:** 3875–3882.

[29] RAMOS N D, CAMPOS T M, PAZ I S, *et al*. Microstructure characterization and SCG of newly engineered dental ceramics. *Dental Materials*, 2016, **32(7):** 870–878.

[30] EKATERINA N, KEYUR K, KIRA C, *et al*. Hall-Petch effect in binary and ternary alumina/zirconia/spinel composites. *Journal of Materials Research and Technology*, 2021, **11:** 823–832.

[31] SENTHIL K, BISWAS P, JOHNSON R, *et al*. Transparent ceramics for ballistic armor applications. *Handbook of Advanced Ceramics and Composites*, 2020, **11:** 435–457.

[32] KRELL A, STRASSBURGER E, HUTZLER T, *et al*. Single and polycrystalline transparent ceramic armor with different crystal structure. *Journal of the American Ceramic Society*, 2013, **96(9):** 2718–2721.

[33] IQBAL M J, ISMAIL B, RENTENBERGER C, *et al*. Modification of the physical properties of semiconducting $MgAl_2O_4$ by doping with a binary mixture of Co and Zn ions. *Materials Research Bulletin*, 2011, **46(12):** 2271–2277.

[34] REN L, WANG H, TU B T, *et al*. Investigation on composition-dependent properties of $Mg_{5x}Al_{23-5x}O_{27+5x}N_{5-5x}$ ($0 \leqslant x \leqslant 1$): Part II. Mechanical properties *via* first-principles calculations combined with bond valence models. *Journal of the European Ceramic Society*, 2021, **41(3):** 4942–4950.